

# The spatial extent of renewable and non-renewable power generation: A review and meta-analysis of power densities and their application in the U.S.

John van Zalk<sup>a</sup>, Paul Behrens<sup>a,b,\*</sup>

<sup>a</sup> Leiden University College, Leiden University, P.O. Box 13228, 2501 EE The Hague, the Netherlands

<sup>b</sup> Institute of Environmental Sciences, Leiden University, P.O. Box 9518, 2300 RA Leiden, the Netherlands



## ARTICLE INFO

### Keywords:

Energy transition  
Spatial impact  
Power density  
Energy systems  
Land  
Energy models

## ABSTRACT

Energy systems are undergoing a significant shift to renewable energy (RE). To date, the surface area required for RE systems is greater than that for non-RE systems, exacerbating existing environmental policy challenges, from increasing land competition, to visual impacts. A suitable metric for comparing the extent of systems is the power density of electricity production, that is, the electrical power produced per horizontal m<sup>2</sup> of surface area. This study systematically reviews power densities for 9 energy-types (wind, solar etc.) and multiple sub-types (e.g., for solar power: PV, solar thermal) in the United States. Median, mean, and uncertainty estimates are provided for 177 different densities from the literature. Non-renewable power densities are found to be three orders of magnitude larger than renewable densities. Natural gas and solar energy yield the highest median density per non-RE, and RE system respectively. Solar energy was the only system to experience a significant, positive relationship in power density over time. We apply these density estimates to NREL scenarios of future energy systems for state-specific assessments, and find that the largest growth in land use is in the southern United States.

## 1. Introduction

Renewable energy (RE) has generally lower power densities than other non-renewable sources (Smil, 2010). That is, RE typically requires more surface area to produce an equivalent amount of power as non-RE system. Given the two-fold importance of land competition and visual impacts, the clean energy transition has led to increasing interest in the spatial impact of energy systems (Bridge et al., 2013; Fouquet, 2016). Smil (2016, 2010) and Mackay (2009a, b), find that future RE systems will cover a significant percentage of available land in the United States and United Kingdom respectively. Smil (2016), highlights that renewables produce energy at a small fraction of current power densities in use in urban areas and industry. Thus, he sees growth in the footprint of the energy sector as inevitable, having to harness renewable flows over extensive areas and in populous centres. In one exploration of a scenario balancing many national concerns, Mackay finds that the production of biofuels would require the majority of available, arable land in the UK (MacKay, 2008). However, other researchers suggest that while the area of energy systems may increase, the growth in land-use by the energy sector would be minor, since RE would be predominantly placed atop existing infrastructure and offshore (most generally rooftop solar, De Boer et al., 2011).

Energy systems modelling can benefit from reliable power density estimates (Brehm et al., 2016; Chiabrand et al., 2009; Delucchi and Jacobson, 2011; Denholm et al., 2000; Honeyman, 2015; Mackay, 2009a, b; NREL, 2012; Sands et al., 2014). Several studies have included spatial implications in long-term market potential, and maximum, production values (Brehm, et al., 2016; Feldman et al., 2015). Studies by Jacobson and Delucchi use power densities to estimate several outcomes in future regional and national energy systems (Delucchi and Jacobson, 2011; Jacobson and Delucchi, 2011). These studies include investigations for meeting energy demands with hydroelectricity, wind, and solar for the world (Jacobson and Delucchi, 2011), and road maps for individual US states (Jacobson et al., 2015). In contrast to other work (MacKay, 2008; Smil, 2010), Jacobson and Delucchi find areas that renewable energy infrastructure would occupy a small fraction of total land available. This has been recently challenged in other works (Clack et al., 2017).

The National Renewable Energy Laboratory (NREL) incorporates power densities to produce estimates of achievable energy generation of each established technology in the U.S. given system performance, topographic limitations, environmental, and land-use constraints (Lopez et al., 2012). For rooftop studies, NREL estimated the percentage of households and buildings that could host PV systems in the United

\* Corresponding author at: Leiden University College, Leiden University, P.O. Box 13228, 2501 EE The Hague, the Netherlands.

E-mail address: [p.a.behrens@luc.leidenuniv.nl](mailto:p.a.behrens@luc.leidenuniv.nl) (P. Behrens).

<https://doi.org/10.1016/j.enpol.2018.08.023>

Received 4 August 2017; Received in revised form 8 August 2018; Accepted 10 August 2018

0301-4215/ © 2018 The Authors. Published by Elsevier Ltd. This is an open access article under the CC BY license (<http://creativecommons.org/licenses/by/4.0/>).

States (Feldman et al., 2015). Gagnon et al. (2016) went further, estimating hosting potential by building size.

Improved understanding of power densities may help examine trade-offs between different land-uses and their social implications. For example Bridge et al. (2013) discuss which types of land will be used more often as renewables gain market penetration, including uplands (wind), narrow sea passages (hydro), and rural environments. Chiabrando et al. (2009) used theoretical power density values in a risk assessment of human vision loss due to glare from a PV system in Italy.

Even though the studies mentioned above use estimates of the spatial extent of power generation, few have compared energy types in a single, standard unit. Layton (2008) determined power densities in  $\text{J}/\text{m}^3$  – giving concentration information, but not surface area requirements. Perhaps the most inclusive estimates have been produced from life-cycle analyses (Fthenakis and Kim, 2010; Gagnon et al., 2002). These estimates compare systems in terms of  $\text{m}^2/\text{Wh}$ . However, they do not incorporate a capacity factor, which for renewables is a serious consideration (given the availability of renewable flows). A more general comparison of surface areas is based on the unit of power – the average electrical power actually transmitted to the grid over some time period (usually a year) in  $\text{W}_e/\text{m}^2$ . Smil (2010) provided high and low estimates for horizontal power density (power density henceforth) by examining the limits of generation arrangements. For example, comparing surface and underground mines for different forms of coal generation.

However, research is lacking on average power density values for energy types and sub-types. It is also not clear whether industries in general trend towards Smil's high or low predictions. Uncertainty estimates are also lacking, precluding the ability of providing further sensitivity estimates in energy system modelling. This paper addresses this knowledge gap by calculating power densities for nine established technologies in the United States including: natural gas, nuclear, oil, coal, solar, wind, geothermal, hydro, and biomass. Within these energy types, the power densities of sub-types are also presented (i.e. switchgrass, palm oil etc.). A literature review is performed, and 177 electric power densities in  $\text{W}_e/\text{m}^2$  from 54 publications are evaluated. Note that although this research focuses on a particular country, the work can be used as an estimate for nations with similar technological and resource availabilities. To investigate whether power densities have changed appreciably over time, implying improving technical implementation, a statistical analysis of developments is conducted. Finally, the power density estimates are applied in an example analysis of two NREL scenarios for the power sector through to 2050. NREL scenarios are chosen since they include national, sub-national, and state-by-state changes in land-use for the power system. To our knowledge this is the first work examining power densities across the literature for different energy types and sub-types.

The article proceeds as follows: Section 3 presents the methods and data used, including the search terms and inclusion criteria; Section 4 presents the results of the meta-analysis and presents visualizations of the land requirements for the electricity sector over time; Section 5 discusses the findings in the context of land and energy policy; Section 5 offers final remarks.

## 2. Methods and data

This study follows PRISMA guidelines for transparent meta-analysis reporting, which are current as of May 2017 (Moher et al., 2015). The databases searched included: Web of Science, Leiden University Catalogue, ScienceDirect, NREL Publications, and GreenFILE. These searches were supplemented using snowball sampling. Works containing the phrase 'power densities' related to other fields such as transportation, medicine, fuel cells, communication devices, buildings, magnetic fields, food chains, etc., were excluded using appropriate search terms. See Appendix Table 1 and Appendix Table 2 for a full list of search terms (including result frequencies) and citations respectively. The

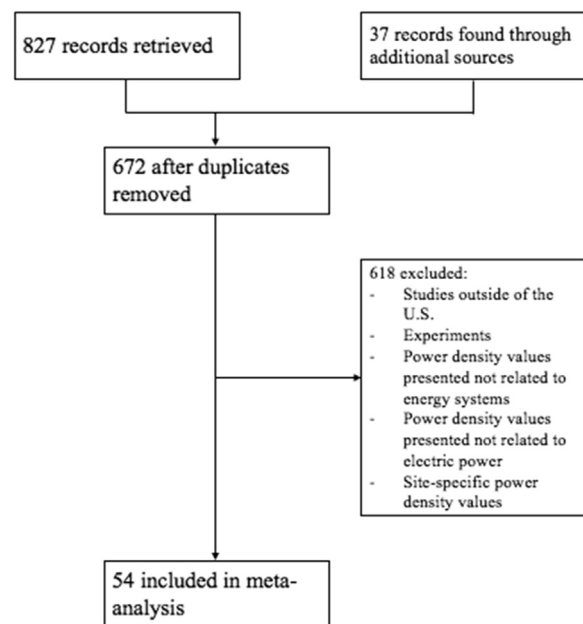


Fig. 1. Flow chart of the selection of eligible studies.

inclusion criteria were that: (1) all publications be in English; (2) all publications except government reports were peer-reviewed; (3) publications giving location-dependent power densities are specific to energy sources or technologies in the U.S.; (4) power densities are for electric power production as opposed to heat generation or liquid biofuel production; and, (5) the publication presents an average or range of power densities rather than one for a specific, individual power plant. This final criterion is important as power densities for specific plants are non-representative since they report experiments rather than developed technologies. Note that there is no time-exclusion criterion in this analysis, because a goal of this study is to examine the change in power densities over time. The earliest paper to feature in this analysis is from 1974. A flow diagram of available studies through the selection process is shown in Fig. 1.

Once the articles were screened, power densities and other details were extracted. Parameters extracted include: publication date, type of energy (e.g. biomass), sub-type within energy type (e.g. switchgrass), power/energy density, the unit reported (e.g. MMBTU), and the type of study (see Appendix Table 3). Additionally, the methods used in each publication were evaluated to determine whether the value accounted for the total footprint (i.e. surface area use in additional infrastructure), efficiency, and/or capacity factor. Finally, the articles were reviewed for citations to other relevant articles in a snowball sampling approach. For articles reporting wind power densities for multiple different wind speeds, the value of the U.S. average (5.5–7.0 m/s) was taken (Archer and Jacobson, 2005; U.S. Environmental Protection Agency, 2013a).

The majority of studies reported power density values which do not represent total footprints, nor did they include efficiencies or capacity factors. These raw power densities were converted to the power density of produced electric power  $PD_e$  in  $\text{W}_e/\text{m}^2$ ,

$$PD_e = PD \times \eta_{eff} \times CF \times infrastructure \quad (1)$$

which incorporates the power density of the resource before conversion  $PD$  (in  $\text{W}/\text{m}^2$ ), the unitless efficiency of the energy converter  $\eta_{eff}$ , the unitless capacity factor  $CF$ , and the unitless infrastructure requirement ratio, which represents the additional surface area required for mines, roads, foundation pads etc. as a ratio of direct surface-area of resource to total surface-area including infrastructure for each energy type. Efficiencies, capacity factor, and infrastructure were taken from the literature and are given in Appendix Table 4, 6, and 9 respectively. For

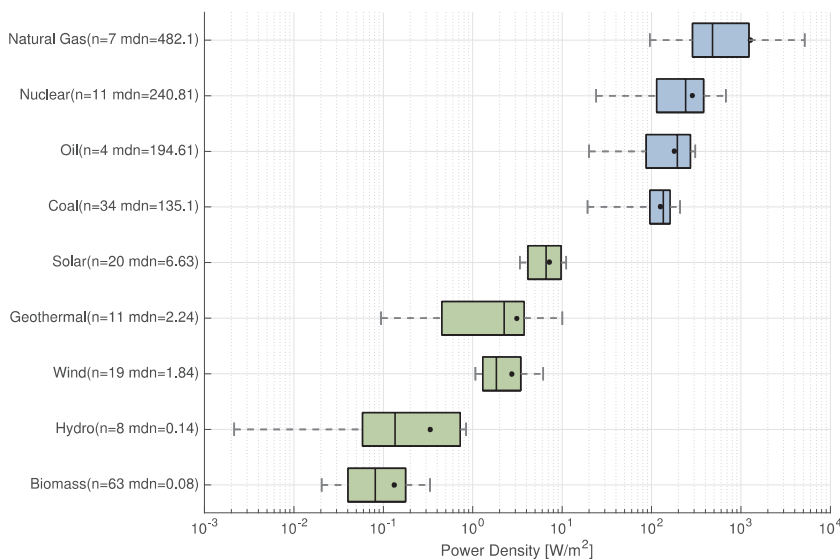


**Fig. 2.** Box plots of power densities for all energy types visualized on a log scale. The annotations *n* and *mdn* give the number of values found for each energy type, and the median power density respectively. Outliers are those values that are further away than 0.5 and 1.5 times the 1st and 3rd quartiles respectively. The round markers show the mean for each energy type. Green boxes are given for renewable energy types, and blue for non-renewable.

illustration, in Gunturu and Schlosser (2012), raw U.S. wind power density was found to be 300–600 W/m<sup>2</sup>; the mean, 450 W/m<sup>2</sup>, was multiplied by a representative efficiency factor for wind power ( $\eta_{eff}$ ) of 0.30 (U.S. Environmental Protection Agency, 2013a, 2013b). Next, this value was multiplied by 0.35 – the average capacity factor (CF) for wind energy in the United States in 2016 (Hankey et al., 2017). Finally, according to Denholm and Margolis (2007), wind turbine foundations themselves comprise 10% of the total area they require given necessary spacing between rotor blades. As such, the value is multiplied by 0.10, yielding a final  $PD_e$  of 4.68 W<sub>e</sub>/m<sup>2</sup>. Each calculation made for each of the values used in the literature are included in the Appendix, Table 3.

For studies that did include capacity factors, the final value was corrected for 2016 capacity factors. If a study included a capacity factor, but did not specify exactly what value was used, it is assumed to be the average capacity factor from the year it was published, then recalculated for 2016. This procedure puts power density values in the context of today's electricity market. This was not possible for older studies including, Bertani (2005), Robeck et al. (1980), Smil (1983), and United States Atomic Energy Commission (1974) where annual average capacity factors are unknown. It was also not possible with specific energy types for Pimentel et al. (1994) and EWG's (2000).

Other studies list volumetric or gravimetric energy densities, in J/m<sup>3</sup> or J/kg respectively, rather than power density values (W/m<sup>2</sup>). These are converted using average values for densities of each fuel type ( $\rho$ ) and yields (see Appendix Tables 6, 7, and 8 for the full list of values) For illustration, Lofthouse et al. (2016) report a volumetric energy density of 0.57 mmbtu/ft<sup>3</sup> for coal. Once converted to SI units (see Appendix, Table 10), this is divided by an average density value of 850 kg/m<sup>3</sup> (Weststeijn, 2002). Next, using an estimated surface area yield of raw coal of 3356.1 kg/m<sup>2</sup>, units of mass are converted to surface areas (Supple, 2013; U.S. Environmental Protection Agency, 2005). Power density is then calculated and multiplied by an  $\eta_{eff}$  of 0.38 and a CF of 0.72 (Hankey et al., 2017; Hussy et al., 2014). Infrastructure requirements reduce the  $PD_e$  by 28% to 140.1 W<sub>e</sub>/m<sup>2</sup> (Smil, 2010).

The primary statistical measures used in reporting are the median (*mdn*), and the mean, with the standard error of the mean ( $\mu \pm SEM$ ). Both are reported as each measure has different advantages in different scenarios.

Next, in order to examine the development of power densities for each energy type over time, a simple linear regression is performed with the model:

$$PD_e = \beta_0 + \beta_1 Year + e \quad (2)$$

where  $\beta_0$  is the intercept,  $\beta_1$  is the gradient, and  $e$  the residual error

between predicted and reported power density values. These regressions are tested for statistically significant deviations from a gradient of 0, indicating no development of power densities over time.

Lastly, in order to show how these values may be applied, and to investigate the change in land-use due to different energy system scenarios, the estimated power densities for different energy types are applied to the National Renewable Energy Laboratory's (NREL) energy scenarios for 2014–2050 (NREL, 2018). The NREL scenarios provide estimates of MWh produced per year for: hydropower, coal, biomass, geothermal, rooftop photovoltaic, utility-scale photovoltaic, concentrated solar power, onshore wind, gas combined cycle, and non-combined cycle gas. Two scenarios are compared, one which meets the 80% RE 2050 target, assuming advanced technology, and a second with a low-demand baseline where natural gas and coal production still dominate the market (see NREL, 2018 for further details). The NREL estimates are disaggregated to the state-level, excluding Alaska and Hawaii.

In order to compute surface area, megawatt-hours are first converted to watts, divided by mean power densities, and converted to hectares for ease of inspection. Large-scale hydropower densities are used here in the knowledge that these make up the majority of US hydro resources (U.S. Department of Energy, 2017). Additionally, the power density for wood crops is used for NREL biomass estimates as it is the dominant source for electricity production in the US (EIA, 2017). The uncertainties in the total estimates are also computed.

Finally, the percentage of state land required for the electricity sector over time is provided, in order to give a basis for comparison. State footprints for both scenarios are combined on a regional and national scales, in order to provide insights into the total, and sub-national impacts of land use for these energy system scenarios.

### 3. Results

First, the aggregated results for all energy types are given, and the underlying trends are introduced (see Fig. 2). Then, the power densities within energy sub-types for renewable and non-renewable resources are examined. The results of the time series regressions and land-use projections are then reported. Finally, the example application of these power densities to future NREL scenarios are presented.

A total of 177 power density values were extracted from 54 studies (all extracted values are available in the Appendix, Table 3). Of these, 56 represented non-renewable sources, and 121 represented renewable sources. One data point was excluded from the analysis as it referenced a mobile gas generator, which is not representative of stationary

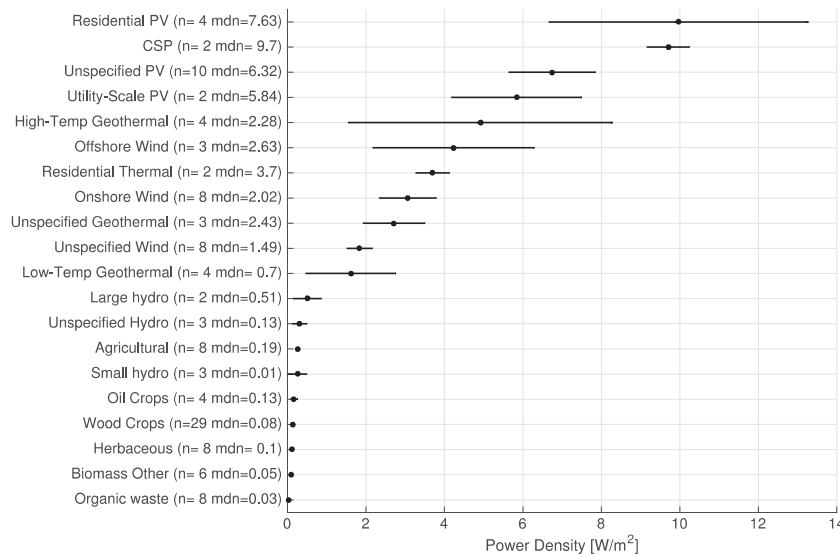


**Fig. 3.** Average  $PD_e$  for renewable energy subtypes with the mean plotted with a round point markers, and the line showing the standard error of the mean. Note the number of samples for each energy subtype in the y axis labels. Where only one value is available the value is plotted with a round marker.

generation. Of the renewable energy types, 63 were for biomass. The power density for all non-renewable types ( $mdn = 145.8 \text{ W}_e/\text{m}^2$ ,  $\mu = 306.9 \pm 102.4 \text{ W}_e/\text{m}^2$ ) was greater than that of renewables ( $mdn = 0.23 \text{ W}_e/\text{m}^2$ ,  $\mu = 2.01 \pm 0.3 \text{ W}_e/\text{m}^2$ ) by more than three orders of magnitude (see Fig. 2). Natural gas systems gave the highest median power densities ( $mdn 482.1 \text{ W}_e/\text{m}^2$ ,  $\mu = 1283.9 \pm 702 \text{ W}_e/\text{m}^2$ ), with the lowest from biomass ( $mdn 0.08 \text{ W}_e/\text{m}^2$ ,  $\mu = 0.13 \pm 0.02 \text{ W}_e/\text{m}^2$ ).

### 3.1. Renewable power densities

Median renewable power densities vary by almost two orders of magnitude, from  $0.08 (\mu = 0.13 \pm 0.02 \text{ W}_e/\text{m}^2)$  for biomass, to  $6.6$  for solar ( $\mu = 7.3 \pm 0.9 \text{ W}_e/\text{m}^2$ ). Fig. 3 shows the mean  $PD_e$  for renewable energy subtypes moving from biomass at the lower end, through to hydropower, wind, geothermal and solar in increasing order.

#### 3.1.1. Hydropower

Power densities of hydropower systems vary extensively, from  $0.008 \text{ W}_e/\text{m}^2$  to  $0.87 \text{ W}_e/\text{m}^2$ , with a median of  $0.14 \text{ W}_e/\text{m}^2$  ( $\mu = 0.34 \pm 0.12 \text{ W}_e/\text{m}^2$ ). The long lower-tail of the boxplot for hydropower in Fig. 2 represents low-power, small-scale projects on local tributaries. Hall (2006) calculated an average power density for these systems of  $0.01 \text{ W}_e/\text{m}^2$  (as low as  $0.0008 \text{ W}_e/\text{m}^2$ , accounting for capacity factor and total footprint). This was the lowest value recorded for any system. Hydroelectric systems in the upper-tail, with values comparable to small wind installations include hydropower systems with reservoirs ( $0.11 \text{ W}_e/\text{m}^2$ , Pimentel, 1994) and run-of-river hydropower installations averaging  $0.75 \text{ W}_e/\text{m}^2$  (Gagnon et al., 2002). Estimates for hydropower with reservoirs include the additional land required for flooding. Large hydropower with reservoirs give a power density of  $\mu = 0.50 \pm 0.25 \text{ W}_e/\text{m}^2$ , albeit with only two estimates. Smaller hydropower installations result in smaller power densities, but with larger uncertainties  $\mu = 0.25 \pm 0.20 \text{ W}_e/\text{m}^2$ .

#### 3.1.2. Wind power

Median wind power density gives a lower value than the mean with  $mdn = 1.84$  compared to  $\mu = 2.73 \pm 0.5 \text{ W}_e/\text{m}^2$ . This may be due overrepresentation of a few exceptional sites in the literature. Differences arise from location, rotor blade size, and turbine height. The first of these factors explains the difference in average power densities for onshore ( $\mu = 3.1 \pm 0.7 \text{ W}_e/\text{m}^2$ ) and offshore farms ( $\mu = 4.2 \pm 1.7 \text{ W}_e/\text{m}^2$ ). Offshore turbine encounter higher winds speeds due to reduced

interference from topography and the built environment (Lu et al., 2009). For articles which do not specify whether estimates are onshore or offshore, values and uncertainties lie lower ( $\mu = 1.8 \pm 0.3 \text{ W}_e/\text{m}^2$ ). According to NREL's Energy Technology Cost and Performance Database, area requirements do not vary greatly between small and medium size wind systems, but there is a substantial increase in the footprint of systems with larger than 1 MW capacity. Part of this increase can be explained by transmission requirements as larger systems are generally located further away from demand.

#### 3.1.3. Geothermal power

Geothermal energy systems vary from  $0.08$  to  $14.94 \text{ W}_e/\text{m}^2$ , with a median of  $2.24 (\mu = 3.1 \pm 1.2 \text{ W}_e/\text{m}^2)$ . Low-temperature and high-temperature resources naturally have different power densities. A threshold of  $250^\circ\text{C}$  was taken, below which systems were classified as low temperature, and above high temperature. High temperature resources have power densities similar to that of wind ( $\mu = 4.9 \pm 2.9 \text{ W}_e/\text{m}^2$ ), whereas Low temperature geothermal results in much lower power densities due to the lower efficiencies involved ( $\mu = 1.6 \pm 1.0 \text{ W}_e/\text{m}^2$ ). In both cases the point estimates have similar standard errors of the mean, resulting in highly uncertain estimates. Where the temperature of the resource was unspecified in the literature, values again lay in between to two extremes, but with smaller standard errors of the mean ( $\mu = 2.7 \pm 0.7 \text{ W}_e/\text{m}^2$ ).

#### 3.1.4. Solar power

Systems vary from  $1.5$  to  $19.6 \text{ W}_e/\text{m}^2$ , with a median of  $6.63 \text{ W}_e/\text{m}^2$  ( $\mu = 7.3 \pm 0.9 \text{ W}_e/\text{m}^2$ ). The solar energy system (Fig. 3) with the lowest power density in the literature was solar thermal ( $\mu = 3.7 \pm 0.3 \text{ W}_e/\text{m}^2$ ), followed by utility-scale PV ( $\mu = 5.8 \pm 1.2 \text{ W}_e/\text{m}^2$ ), residential PV ( $\mu = 6.7 \pm 0.9 \text{ W}_e/\text{m}^2$ ), and concentrated solar ( $\mu = 9.7 \pm 0.4 \text{ W}_e/\text{m}^2$ ) which make up the upper tail of the boxplot in Fig. 2. Residential PV and CSP systems appear to be similar, with the former showing larger uncertainties, possibly due to the diversity of residential systems. Power densities for residential solar calculated here are higher than those for large-scale arrays, or utility-scale systems. This agrees with Delholm and Margolis (2007), who hypothesise that rooftops are already tilted and therefore receive more sunlight than flat panels. Many utility-scale solar installations have south-facing panels, but also require spacing for maintenance.



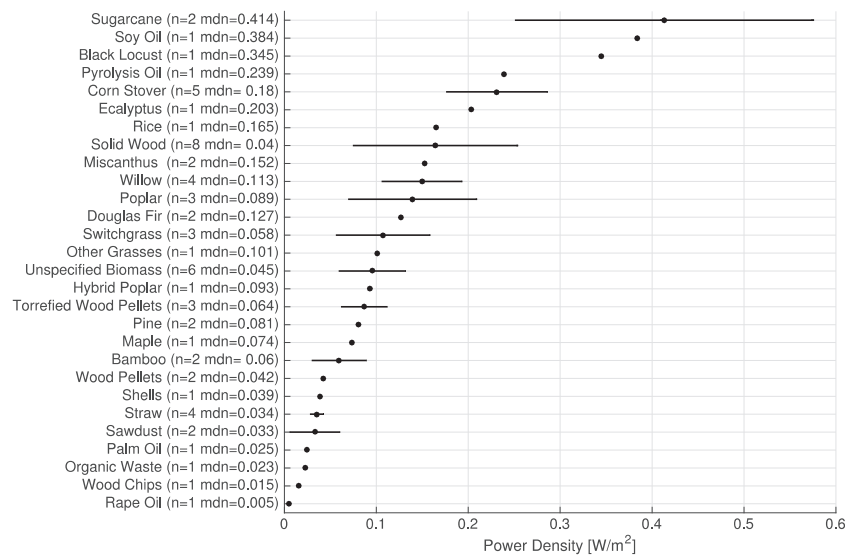


**Fig. 4.** Average  $PD_e$  for Biomass subtypes with the mean plotted with round point markers and the line showing the standard error of the mean. Note the number of samples for each energy subtype in the y axis labels. Where only one value is available the value is plotted with a round marker.

### 3.1.5. Biomass power

Biomass systems have the lowest median power density of  $0.08 \text{ W}_e/\text{m}^2$  ( $\mu = 0.13 \pm 0.02 \text{ W}_e/\text{m}^2$ ), and the lowest maximum power density ( $0.60 \text{ W}_e/\text{m}^2$ ). The most efficient biomass energy sources are sugarcane ( $\mu = 0.42 \pm 0.12 \text{ W}_e/\text{m}^2$ ), soy oil (single estimate,  $0.38 \text{ W}_e/\text{m}^2$ ), black locust (single estimate,  $0.34 \text{ W}_e/\text{m}^2$ ), among other wood crops including eucalyptus (single estimate,  $0.20 \text{ W}_e/\text{m}^2$ ), miscanthus ( $\mu = 0.15 \pm 0.1 \text{ W}_e/\text{m}^2$ ), willow ( $\mu = 0.15 \pm 0.03 \text{ W}_e/\text{m}^2$ ), and poplar ( $\mu = 0.13 \pm 0.04 \text{ W}_e/\text{m}^2$ ). Organic wastes, such as newspaper and other recyclables have the lowest power densities ( $0.03 \pm 0.01 \text{ W}_e/\text{m}^2$ ). See Fig. 4 for an overview of all types.

The efficiency of different biomass energy systems is largely dependent on their bulk densities (see Appendix Table 7). For example, wood chips ( $0.02 \text{ W}_e/\text{m}^2$ ) have a low power density than wood pellets ( $0.04 \text{ W}_e/\text{m}^2$ ) due to the fact that pellets are compressed in industrial processes to achieve higher densities. Pyrolysis oil ( $0.24 \text{ W}_e/\text{m}^2$ ) is also a derivate of solid wood that is produced at high temperatures in the absence of oxygen. In general, solid wood and wood crops have high power densities than herbaceous crops due to higher yields as they grow taller and result in a higher mass-per-unit-of area than herbaceous crops.

## 3.2. Non-renewable power densities

Median renewable power densities in non-renewable systems vary from  $135.1 \text{ W}_e/\text{m}^2$  ( $\mu = 126.6 \pm 12.9 \text{ W}_e/\text{m}^2$ ) for coal, to  $482.1 \text{ W}_e/\text{m}^2$  ( $\mu = 1283.9 \pm 702.0 \text{ W}_e/\text{m}^2$ ) for natural gas. Fig. 5 shows the mean  $PD_e$  for renewable energy subtypes from lignite to natural gas.

### 3.2.1. Natural gas power

Natural gas has the highest power densities (Figs. 2 and 5) of  $mdn$ :  $482.1 \text{ W}_e/\text{m}^2$  ( $\mu = 1283.9 \pm 702.0 \text{ W}_e/\text{m}^2$ ). However, natural gas also has the largest standard error of the mean due to the diversity of the estimates. This diversity is due to differences in opinion of the processes that should be included in the natural gas fuel cycle, namely the decision to include or exclude the land requirements for storage and delivery.

### 3.2.2. Nuclear power

The capacity factors for nuclear are often very high due to technical needs (0.93 in 2016, Hankey et al., 2017). Nuclear power has the second highest power density, with a median power density of  $240.8$

$\text{W}_e/\text{m}^2$  ( $\mu = 288.9 \pm 74.6 \text{ W}_e/\text{m}^2$ ). The extent of the whiskers in Fig. 2 can serve as a proxy of possibilities in efficiency improvements, as they represent the distance from median to maximum achievable power densities. This would likely be made possible by the provision of third generation nuclear that uses fuel more efficiently and creates less waste, reducing power densities by as much as 20% if stored above ground (Marques, 2010; Gagnon et al., 2002).

### 3.2.3. Coal power

Median power densities for coal give  $135.1 \text{ W}_e/\text{m}^2$  ( $\mu = 126.6 \pm 12.9 \text{ W}_e/\text{m}^2$ ). Variations result from differences in coal quality, fuel delivery, and waste disposal. Lignite has the lowest power densities with a median of  $96.1 \text{ W}_e/\text{m}^2$  ( $\mu = 102.4 \pm 11.9 \text{ W}_e/\text{m}^2$ ). Power densities increase from sub-bituminous  $126.7 \text{ W}_e/\text{m}^2$  ( $\mu = 122.4 \pm 8.9 \text{ W}_e/\text{m}^2$ ) and bituminous  $147.0 \text{ W}_e/\text{m}^2$  ( $\mu = 124.4 \pm 23.0 \text{ W}_e/\text{m}^2$ ), to anthracite  $180.9 \text{ W}_e/\text{m}^2$  ( $\mu = 184.2 \pm 12.1 \text{ W}_e/\text{m}^2$ ). Of the 4 lower values, 3 are from life-cycle analyses which, while including direct land impacts similar to other studies, do include some further estimates for waste storage and disposal, as well as off-site combustion (Gagnon et al., 2002; US EWG Group, 2000; AEC, 1974).

### 3.2.4. Oil power

Given the low use of oil for electricity generation in the United States, there are few estimates of its power density. Median power densities give  $194.6$  ( $\mu = 179.5 \pm 53.5 \text{ W}_e/\text{m}^2$ ). Densities range from  $20.0$  to  $308.9 \text{ W}_e/\text{m}^2$  depending on location of processing facilities (onshore vs. offshore), proximity to demand and extent of exploratory drilling required among other activities. Densities in general are driven by a low capacity factor (0.11 in 2016, Hankey et al., 2017).

## 3.3. Variations in power density over time

Of the 9 energy types, solar was the only one to have a significant relationship between power densities and time. Despite having the shortest publication date range, solar shows an estimated increase of  $0.42 \text{ W}_e/\text{m}^2$  per year on average. This may not be surprising given the speed of innovation in the industry. What may be surprising is the lack of a statistically significant trend in wind power densities. While wind does increase over time by an average of  $0.17 \text{ W}_e/\text{m}^2$  per year, it is not a statistically significant trend, mainly due to a number of lower power density estimates in 2009 and 2010. Table 1 shows the results of the

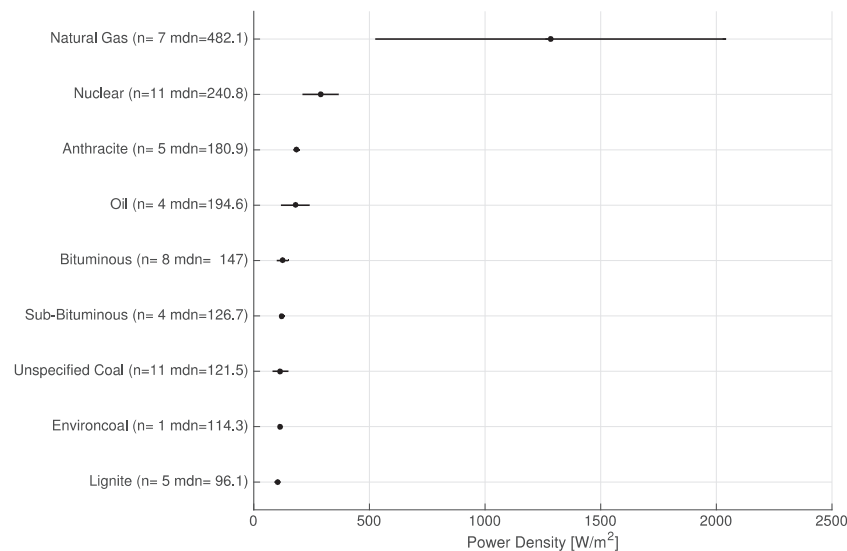


**Fig. 5.** Average  $PD_e$  for non-renewable subtypes with the mean plotted with round point markers and the line showing the standard error of the mean. Note the number of samples for each energy subtype in the y axis labels. Where only one value is available the value is plotted with a round marker.

**Table 1**

Results of regression on power density and time by energy system.

Energy type	n	Publication date range	$\beta_1$	p-value	Significant (p < 0.05)
Natural Gas	7	1974–2010	49.43	0.47	NS
Nuclear	8	1976–2015	5.45	0.47	NS
Oil	4	1974–2008	1.81	0.78	NS
Coal	34	1974–2016	2.36	0.09	NS
Solar	20	1994–2016	0.42	0.001	***
Wind	19	1994–2016	0.13	0.17	NS
Geothermal	11	1987–2015	− 0.12	0.49	NS
Hydro	8	1994–2016	− 0.004	0.87	NS
Biomass	63	1979–2016	− 0.002	0.36	NS

\* n = number of power density values;  $\beta_1$  = slope; Significance codes: “\*\*\*” = 0.001, “\*\*” = 0.01, “\*” = 0.05, “NS” = 0.1 and “NS” = 1.

regression, and Fig. A1 in the Appendix gives the regression plots for the significant result for solar. Natural gas, nuclear, oil, coal and wind show non-negligible, positive, non-significant trends. Geothermal, hydro, and biomass show negative, negligible, non-significant trends.

### 3.4. Land-use of power sector over time

In order to show how these estimates may be applied, and to investigate the change in land-use due to different energy systems, the estimated power densities for energy types are now applied to two NREL scenarios (80% RE by 2050, and a low demand scenario focused on fossil fuels). Applying the power density estimates show that the under the 80% RE scenario, the power sector's footprint is expected to grow by 15 million hectares to 2050 – more than 50% larger than in 2018 (for reference the total land use of the power sector in 2018 is estimated as 20 million hectares, roughly half the size of California). The power sector will occupy 3.66% of total land on the continental United States compared to 44.37% dedicated to agriculture (Food and Agriculture Organization, 2015).

By 2050, the footprint is 40% larger under the 80% RE scenario than the Low-Demand scenario (see Fig. 6). The three main drivers for growth in land-use on the national level is the increase in hydropower, biomass, and onshore wind energy systems, which have the three lowest power densities among systems (see Fig. 7). On the basis of the 80% RE scenario, there is large growth in hydropower until 2020, whereas growth in biomass systems is largely focussed on the decade between 2040 and 2050. The impact from retirement and

decommissioning of coal and natural gas systems is negligible due to their high power-densities.

Next, the changes in land-use are shown for four regions in the U.S., the Midwest, Northeast, South, and West (see Fig. 8). All regions show an increase over time, with the southern United States showing a near tripling in land-use. This is as a result of large-scale biomass generation as well as utility-scale PV, and some hydro. The next largest increases were seen in the West, due to new hydroelectric installations.

Finally, state-specific impacts are shown in Fig. 9 as the percentage of land used in the state (with a maximum of 20% of total available land). Also shown is the breakdown by energy type for 2050. By 2050, the power sector occupies over 15% of the land in 12 states, and over 10% in 9 states. All states experience increases in land-use, with the exception of Michigan and New Hampshire, which experience a short decline over a 2-year period before increasing again thereafter.

At a regional level (as shown on the right side of Fig. 9), there is a sharp contrast in the energy system's land-use between Midwest and Northeast regions. Despite having the least growth in footprint over time, northeastern states' energy systems represent a larger proportion of state land due to the relatively small size of states in that region. In the Midwest, state energy systems required less than 10% of total land. In the far West, many states' footprints are less than 1% of total land.

## 4. Discussion

Renewables currently make up a small share of total U.S. energy production (15%), of which 44% consists of older, hydropower-based resources (EIA, 2017). RE is expected to grow quickly, owing to aggressive renewable energy goals, substitution of other fuels for electricity (generated by RE), and economic forces (EIA, 2017; Zinaman et al., 2012). For some time, it has been understood that this will increase land use requirements for the energy sector. Our results give suggested point estimates and uncertainties of these requirements for each energy type and sub-type. Future land use policy is presented with challenges related to increasing competition, and increasing aesthetic impacts of development. The latter may have a large impact since much of the RE expansion will likely be located near demand on rooftops. Furthermore, as energy systems are expected to shift significantly to further electrification, we may expect land-use to increase in step.

As discussed above, power density estimations have been used in a number of different studies and reports (Brehm et al., 2016; Chiabrando et al., 2009; Delucchi and Jacobson, 2011; Denholm et al., 2000;

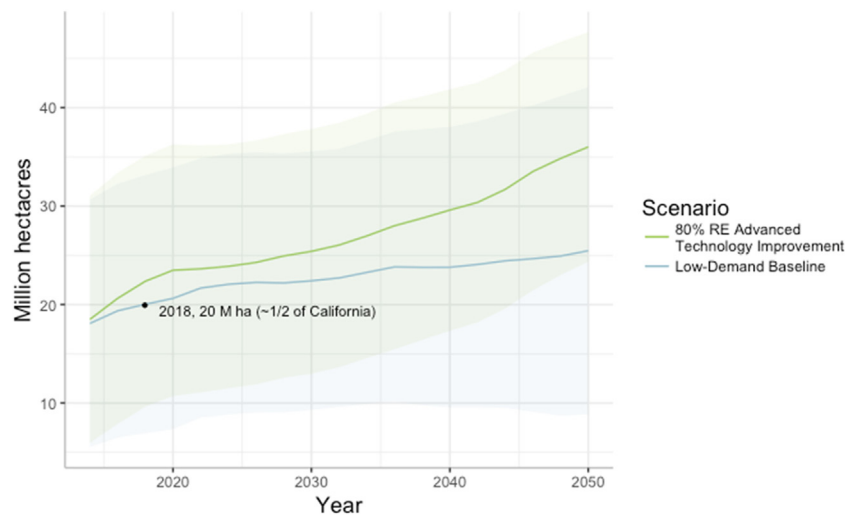


**Fig. 6.** The increase in electricity sector land-use under two NREL scenarios until 2050. For reference the size of California is shown on the figure. The two shaded regions, one in green, and one in blue, show the combined uncertainties using the standard errors of the mean for each energy type.

Honeyman, 2015; Mackay, 2009a, b; NREL, 2012; Sands et al., 2014; Shum, 2017). Accurate values are necessary to assess the feasibility of energy plans and provide further spatial constraints. In Table 2, the results of this study are compared with the limits found by Smil (2016). The estimates for natural gas, coal and solar presented here lie within the ranges of those found by Smil (2016). However, a lower value was calculated for biomass energy systems and a higher value for wind. Smil applies a capacity factor of 70% in calculations for biomass energy systems. This is more than 2 times the current (2016) national average (32%) which is used here (Hankey et al., 2017). Capacity factors also help to explain why estimations for coal sit in the lower end of Smil's interval. Smil uses power densities of 70% and 80% versus the 53% used here. Smil's capacity factors represent values characteristic of the early 2000s. It is worthwhile noting that for some energy types, lower capacity factors may be more appropriate as recent and future energy systems prize flexibility as an important asset. Overall, estimates from this analysis are similar to those found to date, while also incorporating error estimations.

Historic changes in power densities can also serve as an indicator for how they may change in the future. Solar energy systems were the only systems where a significant relationship, positive too, existed between power densities and study publication dates. Solar had the smallest

range in dates of publication (22 years), but had the relationship of highest significance (Table 1). A growth rate of  $0.42 \text{ W}_e/\text{m}^2$  per year was observed, which Smil (2016) suggests can be maintained as three-dimensional PV converters could offer power densities well above  $50 \text{ W}/\text{m}^2$  compared to the  $6.8 \text{ W}/\text{m}^2$  estimate today. Already some researchers are using estimates of 2050 land requirements at  $35 \text{ W}/\text{m}^2$  (Shum, 2017).

The analysis of the spatial extent of energy systems over time featured in this study incorporates proven power densities, and not future trends or improvements. As a result of wide divergence in power densities between RE and non-RE systems, growth in the spatial extent of energy systems occurred in all states on the mainland United States under the 80% RE ATI scenario. States that experienced the largest growth in their footprint generally saw the largest increases in generation across all systems from 2014 to 2050. States with the largest total footprints by 2050 included Vermont and Washington, in which energy systems cover over 20% of available surface area. This high estimate is driven by two main factors, firstly, estimates for hydropower densities vary quite widely across the literature (see Fig. 2) as they are dependent on local geographic and topological constraints. The standard errors are therefore relatively large, and reflective values in these states may be lower if the topology is favourable to hydropower.

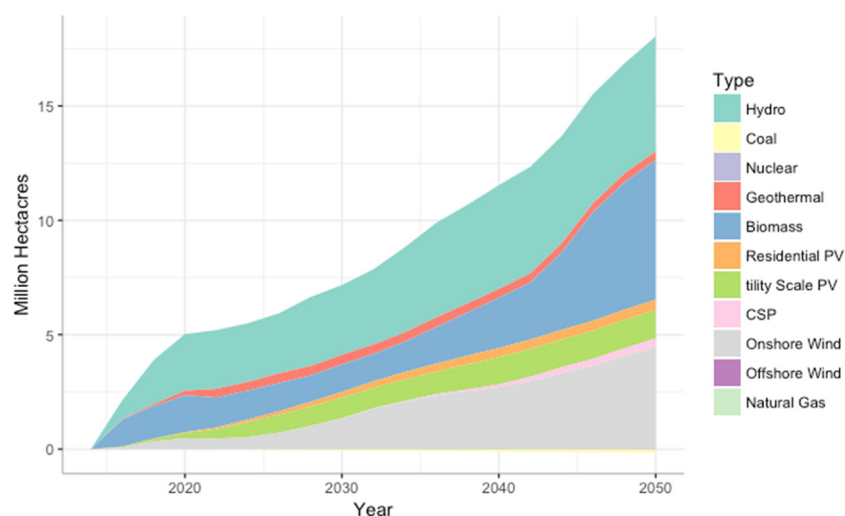


**Fig. 7.** The change in land-use for the electricity system according to the NREL 80% RE scenario. There is a reduction in land use of coal and natural gas, with a small negative contribution.

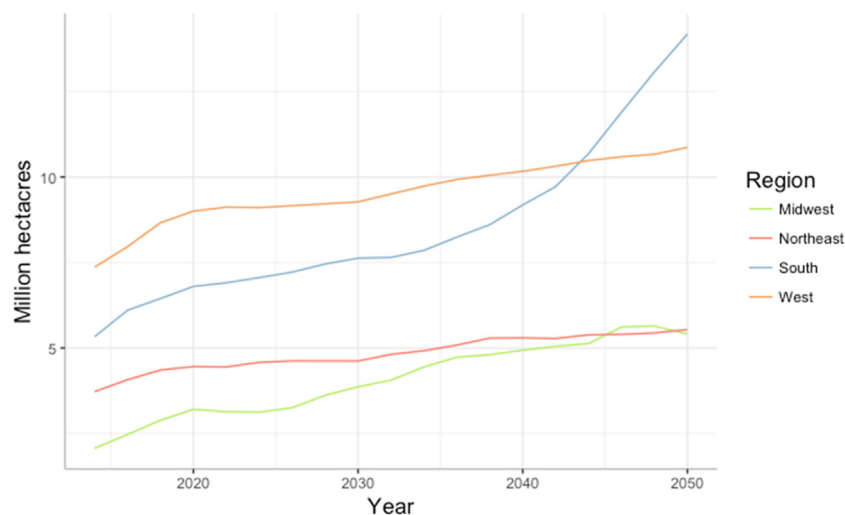


Fig. 8. The change in land-use for the electricity system according to the NREL 80% RE scenario for larger sub-regions of the U.S.

Secondly, and perhaps more importantly, while the NREL scenarios represent cumulative installed capacity by state (and do not consider imports from other countries), they do represent generation installed which is needed for other states. NREL modelling optimizes both costs and resource availability for power generation, and may overrepresent hydropower in states with large hydropower resources. Relatedly, the modelling does not include land use competition and so would not include trade-offs with other sectors such as agriculture. In practise there would be several other factors which would influence whether further hydropower would be built. The values herein give a sense of the scale in terms of the surface area needed for the energy transition.

Increased land-use does not always imply increased competition with other sectors. Oftentimes, land with RE systems can be purposed for multiple uses – the most obvious example being residential PV. Here, energy systems occupy existing infrastructure preserving undeveloped land for other industries. Moreover, biomass energy systems, which have the lowest power densities on average can use agricultural residues or recycled waste, requiring only the addition of a power plant. Given that land occupied by non-RE systems cannot be used for

multiple purposes, it is possible that a RE dominated energy portfolio could reduce land competition on the whole. Nonetheless, whether RE systems occupy developed land or not, they will grow the spatial extent of the power sector. This study does not include enabling technologies such as energy storage which will be vital to RE systems' ability to provide baseload power.

In general, the number of non-renewable power density values was limited to the availability of estimates in the literature, predominately due to the fact they are rarely compared in terms of surface area. Oil in particular has few estimates given its low use in electricity generation. These results are partially dependent on a fewer number of infrastructure estimates from the literature. For example, some estimates may include support buildings, while others do not (Fthenakis and Kim, 2010). This results in large uncertainties and more estimates, transparently reported, would be useful in further studies. Future work could include region-specific power densities due to the variation of renewable resources across the nation. Additionally, yields for newer biomass options are not yet available, and these would be useful for further clarification of the spatial extent of future biomass systems.



Fig. 9. The state-by-state impacts of land-use changes in the electricity system for the 80% RE scenario. To the left of the figure is the variation until 2050, from below 1% of land, to 20% of land. To the right of the figure is the breakdown of electricity types in 2050 for each state and region.



Table 2

Comparison of power density values in prominent literature.

Energy system	Results		n	Smil 2016
	mdn	( $\mu \pm \text{sem}$ )		
Natural Gas	482.1	1283.9 $\pm$ 702	7	200–2000
Coal	135.1	126.5 $\pm$ 12.9	34	100–1000
Unspecified PV	6.6	7.9 $\pm$ 1.5	9	4–9
Solar CSP	9.7	9.7 $\pm$ 0.4	2	4–10
Onshore wind	2.02	3.06 $\pm$ 0.7	8	0.5–1.5
Biomass	0.08	0.13 $\pm$ 0.02	63	0.5–0.6

## 5. Conclusion

Across a large, heterogeneous group of studies, several implications are clear: (1) renewable energy systems differ greatly from non-renewables in power density and (2) increasing the U.S. renewable energy portfolio will increase land-use, presenting challenges for other sectors such as agriculture, and the protection of, for instance, biodiversity. However, the land-use impact of the energy sector can be reduced by the procurement of low-carbon technologies with higher power density values and the multi-purposing of land. This research provides standard errors for these mean estimates, so that future work may include improved sensitivity analysis on land-use. While uncertainties are relatively large, the power density values approximated in this paper represent industry averages in the United States and will be of interest to climate change policy makers, other scientists, and the public.

## Acknowledgements

The Authors would like to thank 4 peer reviewers for their helpful comments and suggestions. P.B. would like to thank the Faber residency in Olot, Spain.

## Appendix A. Supplementary material

Supplementary data associated with this article can be found in the online version at [doi:10.1016/j.enpol.2018.08.023](https://doi.org/10.1016/j.enpol.2018.08.023).

## References

- Archer, C.L., Jacobson, M.Z., 2005. Evaluation of global wind power. *J. Geophys. Res.* 110, D12110. <https://doi.org/10.1029/2004JD005462>.
- Bertani, R., 2005. World geothermal power generation in the period 2001–2005. *Geothermics* 34, 651–690. <https://doi.org/10.1016/j.geothermics.2005.09.005>.
- Brehm, K., Bronski, P., Coleman, K., Doig, S., Goodman, J., Koch Blank, T., Palazzi, T., 2016. Community-Scale Solar: Why Developers and Buyers Should Focus on this High-Potential Market Segment. Washington, DC.
- Bridge, G., Bouzarovski, S., Bradshaw, M., Eyre, N., 2013. Geographies of energy transition: space, place and the low-carbon economy. *Energy Policy* 53, 331–340. <https://doi.org/10.1016/j.enpol.2012.10.066>.
- Chiabrande, R., Fabrizio, E., Garnero, G., 2009. The territorial and landscape impacts of photovoltaic systems: definition of impacts and assessment of the glare risk. *Renew. Sustain. Energy Rev.* 13, 2441–2451. <https://doi.org/10.1016/j.rser.2009.06.008>.
- Clack, C.T.M., Qvist, S.A., Apt, J., Bazilian, M., Brandt, A.R., Caldeira, K., Davis, S.J., Diakov, V., Handschy, M.A., Hines, P.D.H., Jaramillo, P., Kammen, D.M., Long, J.C.S., Morgan, M.G., Reed, A., Sivaram, V., Sweeney, J., Tynan, G.R., Victor, D.G., Weyant, J.P., Whitacre, J.F., 2017. Evaluation of a proposal for reliable low-cost grid power with 100% wind, water, and solar. *Proc. Natl. Acad. Sci. USA* 201610381. <https://doi.org/10.1073/PNAS.1610381114>.
- De Boer, C., Hewitt, R., Bressers, H., Alonso, P.M., Hernández Jiménez, V., Pacheco, J.D., Bermejo, L.R., 2011. Local power and land use: spatial implications for local energy development. *Energy Sustain. Soc.* 5. <https://doi.org/10.1186/s13705-015-0059-3>.
- Delucchi, M.A., Jacobson, M.Z., 2011. Providing all global energy with wind, water, and solar power, Part II: reliability, system and transmission costs, and policies. *Energy Policy* 39, 1170–1190. <https://doi.org/10.1016/j.enpol.2010.11.045>.
- Denholm, P., Hand, M., Jackson, M., Ong, S., 2000. Land-Use Requirements of Modern Wind Power Plants in the United States. Golden, CO.
- Denholm, P., Margolis, R., 2007. The Regional Per-Capita Solar Electric Footprint for the United States. Golden, CO.
- EIA, 2017. Biomass and waste fuels made up 2% of total U.S. electricity generation in 2016 (WWW Document). Today in Energy. URL <https://www.eia.gov/todayinenergy/detail.php?id=33872>.
- Feldman, D., Margolis, R., Brockway, A., Ulrich, E., 2015. Shared Solar: Current Landscape, Market Potential, and the Impact of Federal Securities Regulation. Food and Agriculture Organization, 2015. Agriculture Land (% of Land area) (WWW Document) URL <https://data.worldbank.org/indicator/AG.LND.AGRI.ZS?Locations=US>.
- Fouquet, R., 2016. Historical energy transitions: speed, prices and system transformation. *Energy Res. Soc. Sci.* 22, 7–12. <https://doi.org/10.1016/j.erss.2016.08.014>.
- Fthenakis, V., Kim, H.C., 2010. Life-cycle uses of water in U.S. electricity generation. *Renew. Sustain. Energy Rev.* 14, 2039–2048. <https://doi.org/10.1016/j.rser.2010.03.008>.
- Gagnon, L., Elanger, C.B.I., Uchiyama, Y., 2002. Life-cycle assessment of electricity generation options: the status of research in year 2001. *Energy Policy* 30, 1267–1278.
- Gagnon, P., Margolis, R., Melius, J., Phillips, C., Elmore, R., 2016. Rooftop Solar Photovoltaic Technical Potential in the United States: A Detailed Assessment. Gunturu, U.B., Schlosser, C.A., 2012. Characterization of wind power resource in the United States. *Atmos. Chem. Phys.* 12, 9687–9702. <https://doi.org/10.5194/acp-12-9687-2012>.
- Hankey, R., Cassar, C., Liu, J., Wong, P., Yildiz, O., 2017. Electric Power Monthly with data for March 2017. Washington, DC.
- Honeyman, C., 2015. U.S. Community Solar Market Outlook 2015–2020. Boston, MA.
- Hussy, C., Klaassen, E., Koornneef, J., Wigand, F., 2014. International comparison of fossil power efficiency and CO2 intensity - Update 2014. Utrecht, NL.
- Jacobson, M.Z., Delucchi, M.A., 2011. Providing all global energy with wind, water, and solar power, Part I: technologies, energy resources, quantities and areas of infrastructure, and materials. *Energy Policy* 39, 1154–1169. <https://doi.org/10.1016/j.enpol.2010.11.040>.
- Jacobson, M.Z., Delucchi, M.A., Bazouin, G., Bauer, Z.A.F., Heavey, C.C., Fisher, E., Morris, S.B., Piekutowski, D.J.Y., Vencill, T.A., Yeskoo, T.W., 2015. 100% clean and renewable wind, water, and sunlight (WWS) all-sector energy roadmaps for the 50 United States. *Energy Environ. Sci.* 8, 2093–2117. <https://doi.org/10.1039/c5ee01283j>.
- Layton, B., 2008. A comparison of energy densities of prevalent energy sources in units of joules per cubic meter. *Int. J. Green. Energy* 5, 438–455. <https://doi.org/10.1080/15435070802498036>.
- Lofthouse, J., Simmons, R.T., Yonk, R.M., 2016. Reliability of Renewable Energy: Biomass. Logan, UT.
- Lopez, A., Roberts, B., Heimiller, D., Blair, N., Porro, G., 2012. U. S. Renewable Energy Technical Potentials: A GIS-Based Analysis 40. doi:NREL/TP-6A20-51946.
- Lu, X., McElroy, M.B., Kiviluoma, J., 2009. Global potential for wind-generated electricity. *Proc. Natl. Acad. Sci. USA* 106, 10933–10938. <https://doi.org/10.1073/pnas.0904101106>.
- Mackay, D., 2009a. Sustainable Energy — without the hot air, 1st ed. UIT Cambridge, Cambridge. <https://doi.org/10.1109/PES.2004.1373296>.
- Mackay, D., 2009b. Sustainable Energy — without the hot air, 1st ed. UIT Cambridge, Cambridge. <https://doi.org/10.1109/PES.2004.1373296>.
- Mackay, D., 2008. Sustainable Energy — without the hot air. UIT Cambridge.
- Moher, D., Shamseer, L., Clarke, M., Ghersi, D., Liberati, A., Petticrew, M., Shekelle, P., Stewart, L.A., 2015. Preferred reporting items for systematic review and meta-analysis protocols (PRISMA-P) 2015 statement. *Syst. Rev.* 4, 1. <https://doi.org/10.1186/2046-4053-4-1>.
- NREL, 2018. Renewable Electricity Futures Scenario Viewer [WWW Document]. URL [https://www.nrel.gov/analysis/re\\_futures/data\\_viewer/#](https://www.nrel.gov/analysis/re_futures/data_viewer/#).
- NREL, 2012. Renewable Electricity Futures Study. Golden, CO.
- Pimentel, D., 1994. Renewable Energy: economic and Environmental Issues. *Bioscience* 4, 536–546.
- Robeck, K.E., Ballou, S.W., South, D.W., Davis, M., Chiu, S.Y., Baker, J.E., Dauzvardis, P. A., Carvey, D.B., Torpy, M.F., 1980. Land Use and Energy. Washington DC, USA.
- Sands, R., Schumacher, K., Forster, H., 2014. U.S. CO2 mitigation in a global context: welfare, trade and land use. *Energy J.* 35, 181–197.
- Shum, R.Y., 2017. A comparison of land-use requirements in solar-based decarbonization scenarios. *Energy Policy* 109, 460–462. <https://doi.org/10.1016/j.enpol.2017.07.014>.
- Smil, V., 2016. Power Density: a Key to Understanding Energy Sources and Uses. MIT Press.
- Smil, V., 2010. Power Density Primer: Understanding the Spatial Dimension of the Unfolding Transition to Renewable Electricity Generation (Part I – Definitions). Smil, V., 1983. Biomass. In: Biomass Energies. Springer US, Boston, MA, pp. 1–19. [https://doi.org/10.1007/978-1-4613-3691-4\\_1](https://doi.org/10.1007/978-1-4613-3691-4_1).
- Supple, D., 2013. Units & Conversion Factors [WWW Document]. Massachusetts Inst. Technol.
- U.S. Department of Energy, 2017. Types of Hydropower Plants (WWW Document). URL <https://www.energy.gov/eere/water/types-hydropower-plants>.
- US Environmental Working Group, 2000. Choosing Green Energy: A Consumer's Guide to Sustainable Electricity [WWW Document]. <https://www.ewg.org/research/environmental-impacts/source-ratings#land>.
- U.S. Environmental Protection Agency, 2013a. Renewable Energy Fact Sheet: Wind Turbines.
- U.S. Environmental Protection Agency, 2013b. Wind Turbines. Renew. Energy Fact Sheet.
- U.S. Environmental Protection Agency, 2005. U.S. Surface Mines Emissions Assessment. United States Atomic Energy Commission, 1974. Comparative Risk-Cost-Benefit Study of Alternative Sources of Electrical Energy. Washington DC, USA.
- Weststeijn, A., 2002. RE: Optimizing Fuel Volume Density. Renewable Energy Policy Project (WWW Document). Bioenergy Arch. Febr. 2001. URL [http://www.bioenergylists.org/stovesdoc/Weststeijn/Optimizing\\_Fuel\\_Density.PDF](http://www.bioenergylists.org/stovesdoc/Weststeijn/Optimizing_Fuel_Density.PDF) (Accessed 26 May 2017).
- Zinaman, O., Mai, T., Lantz, E., Gelman, R., Porro, G., 2012. ReEDS Modeling of the President's 2020 U.S. Renewable Electricity Generation Goal.